

First-Principles Calculations of Luminescence Spectrum Line Shapes for Defects in Semiconductors: The Example of GaN and ZnO

Audrius Alkauskas, John L. Lyons, Daniel Steiauf, and Chris G. Van de Walle
 Materials Department, University of California, Santa Barbara, California 93106-5050, USA
 (Dated: March 14, 2013)

We present a theoretical study of broadening of defect luminescence bands due to vibronic coupling. Numerical proof is provided for the commonly used assumption that a multi-dimensional vibrational problem can be mapped onto an effective one-dimensional configuration coordinate diagram. Our approach is implemented based on density functional theory with a hybrid functional, resulting in luminescence lineshapes for important defects in GaN and ZnO that show unprecedented agreement with experiment. We find clear trends concerning effective parameters that characterize luminescence bands of donor- and acceptor-type defects, thus facilitating their identification.

PACS numbers: 63.20.kp, 61.72.Bb, 71.55.-i, 78.55.Cr

Defects play a key role in the properties of solids. From the early days of color centers, the study of luminescence and absorption has been crucial to defect characterization [1]. Theoretical efforts to calculate the broadening of optical transitions at defects due to the interactions with lattice vibrations were pioneered by Huang and Rhys [2] and Pekar [3]. While those theories and their generalizations [1, 4] have been very successful in describing the shape of experimental optical bands [1, 5], this inevitably required the use of empirical fitting parameters. Theory has thus been limited in its ability to aid the microscopic identification of defects or produce accurate predictions.

In this Letter we report that unprecedented precision can now be achieved by rigorously mapping the multi-dimensional vibrational problem onto an effective one-dimensional configuration coordinate diagram, combined with advanced electronic structure techniques [6, 7]. We demonstrate the power of the approach with the example of a number of defects in GaN [5] and ZnO [8], two technologically crucial wide-band-gap semiconductors. Excellent agreement with experiment is achieved for well-characterized defects, and new insights into vibronic coupling emerge.

Our electronic structure calculations are based on density functional theory using the hybrid functional of Ref. [7] in the VASP code [9]. The fraction α of the screened Fock exchange admixed to the semilocal exchange was set to 0.31 for GaN and 0.36 for ZnO to reproduce experimental band gaps (3.5 eV and 3.4 eV). By describing bulk electronic structure better and reducing self-interaction errors, hybrid functionals substantially improve the accuracy of defect calculations [10–12]. Defects were treated via the supercell approach [6], the interaction with nuclei was described within the projector-augmented wave formalism [9], and electron wave functions were expanded in plane waves with a cutoff of 400 eV. Normal modes and frequencies have been calculated using finite differences.

We illustrate the methodology with the example of the Mg_{Ga} acceptor in GaN, a crucial defect since it is the only acceptor impurity capable of making the material

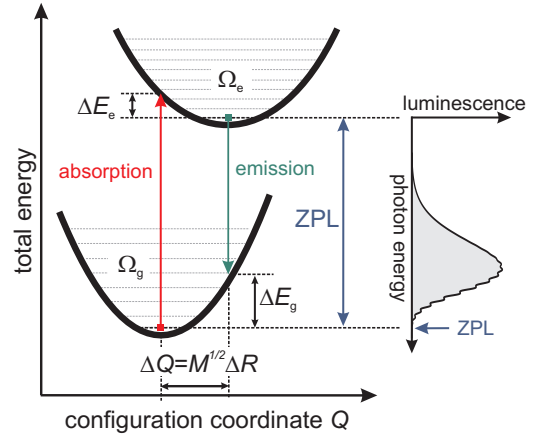


FIG. 1: (Color online) 1D configuration coordinate diagram describing optical absorption and emission at a point defect. The minima of the ground-state and excited-state potential energy surfaces are displaced. $\Delta E_{\{e,g\}}$ are the relaxation energies and $\Omega_{\{e,g\}}$ the effective phonon frequencies. ZPL indicates the zero-phonon line, i.e. the transition between the zero-point vibrational states in excited and ground-state configurations.

p type. While *electrically* acting as a shallow impurity with modest ionization energy, *optically* Mg_{Ga} behaves as a deep center [13]: recombination of an electron at the conduction-band minimum (CBM) with a hole localized on the neutral Mg_{Ga}^0 acceptor gives rise to a broad blue luminescence band [5, 13]. The calculated zero-phonon line (ZPL) energy (see Fig. 1) is 3.24 eV. We assume here that optical transitions start with a delocalized charge carrier; excitonic effects are small [14].

The general theory of luminescence was described in Refs. [1, 2, 4]. When optical transitions are dipole-allowed, as is the case for the defects studied in this work, at $T=0$ the normalized luminescence intensity (lineshape) in the leading order (the Franck-Condon approximation) can be written as $G(\hbar\omega) = C\omega^3 A(\hbar\omega)$,

where $A(\hbar\omega)$ is the normalized spectral function

$$A(\hbar\omega) = \sum_n |\langle \chi_{e0} | \chi_{gn} \rangle|^2 \delta(E_{\text{ZPL}} - \hbar\omega_{gn} - \hbar\omega), \quad (1)$$

and $C^{-1} = \int A(\hbar\omega) \omega^3 d(\hbar\omega)$. The sum runs over all vibrational levels with energies $\hbar\omega_{gn}$ of the ground state, χ are ionic wavefunctions, and E_{ZPL} is the energy of the ZPL. Generalization to finite T is straightforward.

Evaluation of $A(\hbar\omega)$ is complicated by the fact that, first, the sum includes all relevant vibrational degrees of freedom, and second, normal modes \mathbf{Q}_e and \mathbf{Q}_g in the excited and the ground state are usually not identical. The two are related via the Duschinsky transformation $\mathbf{Q}_e = \mathbf{J}\mathbf{Q}_g + \Delta\mathbf{Q}$ [15], and $\langle \chi_{e0} | \chi_{gn} \rangle$ are thus highly-multi-dimensional integrals. For small molecular systems recursive techniques to calculate such integrals have been developed [16] and implemented [17]. The large number of vibrational modes that occur for defects in solids render such a direct approach computationally prohibitive.

Broad optical bands have most often been described via 1D configuration-coordinate diagrams (CCDs) [1, 4] [Fig. 1], based on the assumption that the large number of vibrational modes (with different frequencies) contributing to the lineshape can be replaced by a single effective mode (sometimes a small number of modes). The parameters entering the 1D model are the modal mass M of the effective vibration, the displacement of the potential energy minima ΔR , and the effective frequencies Ω_g and Ω_e [Fig. 1]. Based on these, the widely used ‘‘Huang-Rhys (HR) factors’’ [2] are defined as the average number of phonons created during a vertical transition: $S_g = \Delta E_g / \hbar\Omega_g$ and $S_e = \Delta E_e / \hbar\Omega_g$. There are many examples where a 1D model with empirical fitting parameters provides a good approximation to experimental luminescence lineshapes [1, 5]; still, because it is strictly valid only when all the modes have the same frequency [2], its general applicability has often been questioned. More importantly, the use of fitting parameters precludes linking to potentially valuable microscopic information about the defect and limits the predictive power.

Here we address this problem using the following strategy. Vibrations that couple strongly to the distortion of the geometry are expected to be dominant in $A(\hbar\omega)$. Such modes have finite weight on the atoms that experience the largest relaxations, i.e., the atoms close to the defect. When only a small number of atoms are included, $\langle \chi_{e0} | \chi_{gn} \rangle$ can be evaluated exactly, taking mode mixing into account [16, 17]. This exact evaluation can then serve as a test of the accuracy of any approximations. Once an approximate treatment has been validated in this fashion, it can be applied to much larger systems of atoms provided it is sufficiently less numerically demanding than the exact evaluation.

In the case of Mg_{Ga}^0 a hole is localized on a N neighbor of the Mg atom, and the five atoms surrounding this hole account for more than 90% of the whole relaxation.

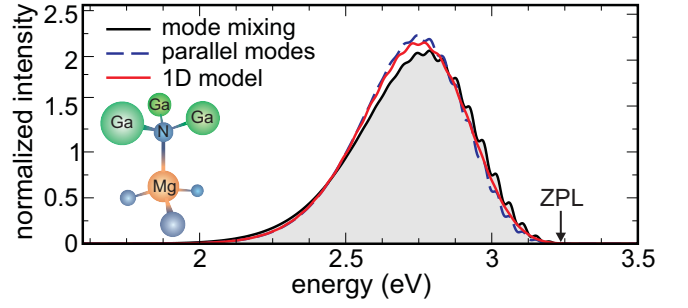


FIG. 2: (Color online) Normalized luminescence spectrum of the $\text{Mg}_{\text{Ga}}(0/-)$ transition, calculated taking into account vibrational modes of only those atoms that relax most (labelled in the inset). Black solid line (and shaded area): calculation including mode mixing; blue dashed line: parallel-mode approximation; red solid line: effective 1D vibrational problem.

The calculated luminescence lineshape, taking mixing between the resulting 15 vibrations into account, is shown in Fig. 2. Multi-dimensional overlap integrals were calculated using the MOLFC code [17]. We have applied a Gaussian smearing with a small $\sigma=0.01$ eV to simulate additional broadening mechanisms, resulting in a smooth lineshape.

Recursive algorithms [16] lead to exploding computational requirements when applied to larger atom clusters. A simplification that is often used for molecules [17] and almost always implied in solids [4] is the parallel-mode approximation, in which the eigenmodes of either the ground state or the excited state are chosen as common vibrational states, leading to $\mathbf{J}=\mathbf{1}$. $\langle \chi_{e0} | \chi_{gn} \rangle$ then factorizes into 1D integrals, each corresponding to one vibrational mode, greatly reducing computational complexity. As seen in Fig. 2, the resulting lineshape is indeed close to the exact result. Therefore, while mode mixing is present, it is not substantial.

Now that we have validated the parallel-mode approximation we can include more atoms, since overlap integrals become easy to calculate. However, the number of terms that have to be included grows very rapidly with system size. This reflects the fact that important modes often do not occur in the gap of the bulk phonon spectrum but are resonances, and therefore not well localized in real space. Consequently, further approximations are required. This we achieve by devising a suitable 1D CCD based on computed parameters as outlined below.

The weight by which each normal mode k contributes to the distortion of the defect geometry during optical transition can be written as $p_k = (\Delta Q_k / \Delta Q)^2$, where

$$\Delta Q_k = \sum_{\alpha i} m_{\alpha}^{1/2} \Delta R_{\alpha i} q_{k;\alpha i}; (\Delta Q)^2 = \sum_k \Delta Q_k^2. \quad (2)$$

Here α labels atoms, $i=\{x, y, z\}$, $\Delta R_{\alpha i} = R_{e;\alpha i} - R_{g;\alpha i}$ is the distortion vector, $R_{\{e,g\};\alpha i}$ are atomic coordinates, and $q_{k;\alpha i}$ is the unit vector in the direction of the normal

mode k ($\sum_{\alpha i} q_{k;\alpha i} q_{l;\alpha i} = \delta_{k,l}$). We find that it is useful to define an effective frequency

$$\Omega_{\{e,g\}}^2 = \langle \omega_{\{e,g\}}^2 \rangle = \sum_k p_{\{e,g\};k} \omega_{\{e,g\};k}^2, \quad (3)$$

where $\omega_{\{e,g\};k}$ is the frequency of the mode $q_{\{e,g\};k}$.

Parameters E_{ZPL} , ΔQ , Ω_g and Ω_e define a 1D CCD (cf. Fig. 1) for a quantum oscillator with unit mass and can be used to calculate the luminescence lineshape. Gaussian smearing is still applied, but it should now reflect the replacement of many vibrations at various frequencies with one effective frequency. Inspection of the mean-square deviation for the distribution of phonon frequencies that contribute to the distortion leads to $\sigma=0.025$ eV ($\sim 0.6\hbar\Omega_g$). The result for Mg_{Ga} in Fig. 2 shows that our rigorously defined 1D model is an excellent approximation to the multi-dimensional calculations.

Now that the validity of the 1D model has been established, it can be extended to larger numbers of atoms and we no longer need to explicitly calculate normal modes and frequencies to determine the effective parameters ΔQ [Eq. (2)] and $\Omega_{\{e,g\}}$ [Eq. (3)]. Indeed, by inserting the expression for ΔQ_k into the one for ΔQ in Eq. (2), one can show that when all the atoms in the supercell are included in the vibrational problem, $(\Delta Q)^2 = \sum_{\alpha,i} m_{\alpha} \Delta R_{\alpha i}^2$. The modal mass is defined via $\Delta Q = M^{1/2} \Delta R$, where $(\Delta R)^2 = \sum_{\alpha,i} \Delta R_{\alpha i}^2$. Effective frequencies Ω can be obtained by mapping the potential energy surface around the respective equilibrium geometries along the path that linearly interpolates between the two geometries [18]. A third-order polynomial fit was found to suffice in all cases. The frequency Ω in the quadratic term defined in this way is equivalent to the one calculated from Eq. (3). Third-order anharmonic corrections that affect vibrational wavefunctions and thus overlap integrals, were included in the calculations of the spectral function perturbatively. For all subsequent calculations, we have used 96-atom wurtzite supercells, and relaxations of all the atoms were included in determining effective parameters. The resulting parameters are summarized in Table I.

The luminescence lineshape $G(\hbar\omega)$ for Mg_{Ga} at $T=0$ K is shown in Fig. 3(a), together with experimental low-temperature data from Refs. [19] and [20]. To facilitate comparison with experiment, the calculated lineshapes were shifted to bring the maximum of the luminescence in agreement with that of the experimentally measured curves. The magnitude of the shift provides an estimate for the error in the E_{ZPL} (thermodynamic transition level), and is less than 0.1 eV for all defects. This error bar reflects both the remaining inaccuracy of even the most advanced first-principles methods, and any electrostatic corrections (such as excitonic effects or donor-acceptor interactions) not included in the present model. The width of the theoretical band (0.44 eV) is

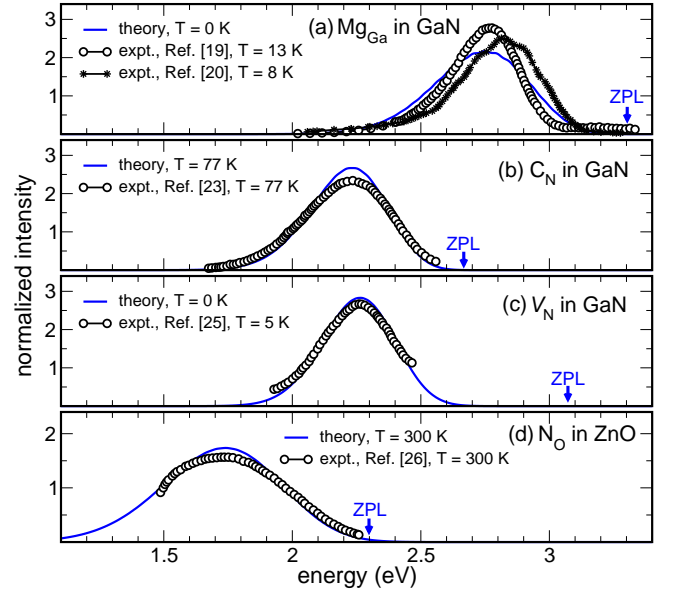


FIG. 3: (Color online) Calculated (solid lines) and measured (symbols) luminescence lineshapes for various defects in GaN and ZnO. (a) Mg_{Ga} in GaN, expt. from Refs. [19] (disks) and [20] (stars) (b) C_N in GaN, expt. from Ref. [23]; (c) V_N in GaN, expt. from Refs [25]. (d) N_O in ZnO, expt. from Ref. [26] The arrows indicate the ZPL, and the calculated spectra were shifted by ~ 0.1 eV, as discussed in the text.

only slightly larger than the experimental value of 0.36–0.37 eV. We derive the effective vibrational frequency in the ground state $\Omega_g=47$ meV, and the HR factor $S_g=12$. The good agreement between the calculated and experimental lineshapes for Mg_{Ga} attests to the power of the approach presented here, when used in combination with state-of-the-art density functional calculations.

The agreement with experiment is even better for our second example, C_N . This defect has been suggested as a source of yellow luminescence (YL) [5, 22, 23] based on the transition $C_N^0 + e^- \rightarrow C_N^-$ [21] (where e^- is an electron at the CBM). This defect again exhibits hole localization in the neutral charge state, but now the hole is localized on the C atom [21]. The calculated luminescence lineshape at $T=77$ K [Fig. 3(b)] agrees very well with the measurements of Ref. [23], in which YL was convincingly attributed to a C-related defect. Our calculated effective frequencies ($\hbar\Omega_{\{e,g\}}=36, 42$ meV) and HR factors ($S_{\{e,g\}}=10, 11$) are in an excellent agreement with those measured in Ref. [22] (Table I).

Our next example is V_N . Nitrogen vacancies have low formation energies in p -type GaN, and they have been suggested [24] as a cause of the YL in p -GaN observed in Ref. [25]. The calculated luminescence lineshape for the transition $V_N^{+3} + e^- \rightarrow V_N^{+2}$ [Fig. 3(c)] shows impressive agreement with these low-temperature experiments.

To demonstrate that the approach is not limited to GaN, in Fig. 3(d) we compare the calculated and mea-

TABLE I: Effective parameters for various defect-related luminescence transitions in GaN and ZnO. ΔQ and ΔR : total mass-weighted and total distortions; M : modal mass; $\Omega_{\{e,g\}}$: effective frequencies in the ground and excited states (charge state in parentheses); E_{ZPL} : zero-phonon line energy; FWHM: full-width at half maximum of the band; T: temperature for which the FWHM is given; $S_{\{e,g\}}$: Huang-Rhys factors. If experimental parameters are not explicitly given in the corresponding experimental papers, they are extracted using the original data and are shown in italics.

Defect, charge states, and optical transition	Method	ΔQ (amu ^{1/2} Å)	M (amu)	ΔR (Å)	$\hbar\Omega_g$ (meV)	$\hbar\Omega_e$ (meV)	E_{ZPL} (eV)	FWHM at T (eV, K)	S_g	S_e
Mg _{Ga} (0/-) in GaN	theory	1.6	45	0.24	47 (-)	34 (0)	3.24 [13]	0.44 at 0	12	-
Mg _{Ga} ⁰ + e ⁻ → Mg _{Ga} ⁻	expt.						<i>3.30</i> [19]	<i>0.36</i> at 13 [19]		
C _N (0/-) in GaN	theory	1.6	51	0.22	42 (-)	36 (0)	2.60 [21]	0.35 at 77	11	10
C _N ⁰ + e ⁻ → C _N ⁻	expt.				41±5	40±5 [22]	2.64 [22]	<i>0.39</i> at 77 [23]	12.8±1.6	13.4±1.7 [22]
V _N (+3/+2) in GaN	theory	3.7	68	0.45	23 (+2)	21 (+3)	3.02 [24]	0.33 at 0	36	35
V _N ⁺³ + e ⁻ → V _N ⁺²	expt.						<i>3.07</i> [25]	<i>0.36</i> at 5 [25]		
N _O (0/-) in ZnO	theory	1.9	48	0.28	40 (-)	32 (0)	2.20 [12]	0.54 at 300	15	15
N _O ⁰ + e ⁻ → N _O ⁻¹	expt.						<i>2.30</i> [26]	<i>0.55</i> at 300 [26]		

sured [26] luminescence lineshapes at $T=300$ K for the deep N_O acceptor in ZnO, corresponding to the transition N_O⁰ + e⁻ → N_O⁻¹ [12]. The agreement between theory and experiment is again extremely good.

Our ability to calculate accurate parameters allows us to examine some general trends. For the two substitutional acceptors in GaN analyzed above, total distortions ΔR amount to 0.22 – 0.24 Å, and HR factors to 10 – 12, irrespective of whether the hole is bound to C or N. Other acceptors with anion-bound holes (V_{Ga}, Be_{Ga}, Zn_{Ga}) show very similar behavior. The donor V_N, on the other hand, is very different. Its defect wave function is composed mainly of Ga 4s states, and ΔR associated with the (+3/+2) transition is 0.45 Å, almost twice as large as in the case of acceptors. The distortion mostly affects the four nearest Ga atoms, leading to a large modal mass and small effective frequencies (Table I). In conjunction with large relaxation energies (0.72 and 0.82 eV) this results in very large HR factors ($S_{\{e,g\}} = 35, 36$). This is in contrast with the acceptors, where anions are involved in the distortion, leading to a smaller modal masses, higher effective vibrational frequencies, and hence smaller HR factors. Similar trends are observed for ZnO: we find $\hbar\Omega_{\{e,g\}}=28\text{--}40$ meV and $S_{\{e,g\}}=15\text{--}23$ for acceptors with anion-localized holes (N_O, V_{Zn}, Li_{Zn}) while $\hbar\Omega_{\{e,g\}}=16, 21$ meV and $S_{\{e,g\}}\approx 50$ for donors with cation-derived states (V_O). The general result for acceptors in ZnO is in accord with experimental data of Ref. 27.

While such *a posteriori* interpretations are simple and intuitive, they are only reliable if based on an accurate microscopic description of the defect. We note that model calculations have yielded results that were very different from our first-principles values (e.g., $S=3.5\text{--}6.5$ for defects related to YL in Ref. [28]), starkly illustrating the shortcomings of such approaches.

High values of HR factors mean that it is very difficult to determine the ZPL in experimental luminescence spectra. Indeed, the weight of the ZPL is exponentially sup-

pressed for larger S : $|\langle\chi_{e0}|\chi_{g0}\rangle|^2 \approx \exp\{-S_{\{e,g\}}\}$ (equality holds for $\Omega_g = \Omega_e$ [2]). As seen in Fig. 3, such complication arises for all the defects studied here and is especially apparent for V_N. This highlights the practical use of calculations exemplified in the current work.

The examples have demonstrated that our methodology is capable of producing luminescence lineshapes in very good agreement with experiment, as well as quantities that can be directly compared with experimental parameters. The achieved agreement is based, of course, on the accuracy of the underlying electronic structure method, but also on the applicability of the 1D model to broad luminescence bands. While the explicit consideration of many vibrational modes is sometimes needed to understand the experimental spectra when $S \approx 01$ (i.e., defects with moderate electron-phonon coupling) [1, 4, 29], We have demonstrated that such a model, with suitably calculated parameters, is indeed valid for defects with large electron-phonon coupling ($S \gg 1$), even if many phonon modes couple to the optical transition. Another important conclusion that follows from our work is that the effective mode frequency is usually much smaller than that of LO phonons (91 meV in GaN and 73 meV in ZnO), contrary to what has been commonly assumed in phenomenological approaches [2]. Our conclusion is in full agreement with detailed experimental measurements for color centers in alkali halides [30], indicating the generality of the obtained result.

Our findings are important for future studies of semiconductors and insulators that exhibit broad defect luminescence bands. In particular, as our examples showed the methodology provides a means for identifying the microscopic origin of the numerous as yet unassigned luminescence bands in technologically important wide band-gap materials. More generally, our work attests to the success of first-principles methods to describe electron-phonon interactions in solids [31] beyond the application to perfect crystals.

We thank F. Bechstedt, N. Grandjean, A. Janotti, M. A. Reshchikov, and Q. Yan for discussions, as well as A. Borelli for a copy of the MOLFC code. AA acknowledges a grant from the Swiss NSF (PA00P2_134127). Additional support was provided by NSF (DMR-0906805), and computational resources by XSEDE (NSF DMR07-0072N) and NERSC (DOE Office of Science DE-AC02-05CH11231).

-
- [1] A. M. Stoneham, *Theory of Defects in Solids* (Oxford University Press, 1975).
 - [2] K. Huang and A. Rhys, Proc. Royal Soc. **204**, 406 (1950).
 - [3] S. I. Pekar, Zh. Expt. Th. Phys. **20**, 510 (1950).
 - [4] M. Lax, J. Chem. Phys. **20**, 1752 (1952); J. J. Markham, Rev. Mod. Phys. **31**, 956 (1959); I. S. Osad'ko, Physics Uspekhi **128**, 21 (1979).
 - [5] M. A. Reshchikov and H. Morkoç, J. Appl. Phys. **97**, 061301 (2005).
 - [6] C. G. Van de Walle and J. Neugebauer, J. Appl. Phys. **95**, 3851 (2004).
 - [7] J. Heyd, G. E. Scuseria, and M. Ernzerhof, J. Chem. Phys. **118**, 8207 (2003).
 - [8] U. Özgür *et al.*, J. Appl. Phys. **98**, 041301 (2005).
 - [9] G. Kresse and J. Furthmüller, Phys. Rev. B **54**, 11169 (1996); G. Kresse and J. Joubert, Phys. Rev. B **59**, 1758 (1999).
 - [10] G. Pacchioni, F. Frigoli, D. Ricci, and J. A. Weil, Phys. Rev. B **63**, 054102 (2000).
 - [11] A. Alkauskas, P. Broqvist, and A. Pasquarello, Phys. Rev. Lett. **101**, 046405 (2008); Phys. Status Solidi B **248**, 775 (2011).
 - [12] J. L. Lyons, A. Janotti, and C. G. Van de Walle Appl. Phys. Lett. **95**, 252105 (2009).
 - [13] J. L. Lyons, A. Janotti, and C. G. Van de Walle, Phys. Rev. Lett. **108**, 156403 (2012).
 - [14] The exciton binding energy in bulk GaN is 0.021-0.023 eV, as measured in W. Shan *et al.*, Phys. Rev. B **54**, 16369 (1996).
 - [15] F. Duschinsky, Acta Physiochim. USSR **7**, 551 (1937).
 - [16] E. V. Doktorov, I. A. Malkin, and V. I. Man'ko, J. Mol. Spectrosc. **64**, 302 (1977).
 - [17] R. Borrelli and A. Peluso, J. Chem. Phys. **119**, 8437 (2003).
 - [18] F. Schanovsky, W. Gös, and T. Grasser, J. Vac. Sci. Technol. B **29**, 01A201 (2011).
 - [19] M. A. Reshchikov, G.-C. Yi, and B. W. Wessels, Phys. Rev. B **59**, 13176 (1999).
 - [20] M. Leroux, N. Grandjean, B. Beaumont, G. Nataf, F. Semond, J. Massies, and P. Gibart, J. Appl. Phys. **86**, 3721 (1999).
 - [21] J. L. Lyons, A. Janotti, and C. G. Van de Walle, Appl. Phys. Lett. **97**, 152108 (2010).
 - [22] T. Ogino and M. Aoki, Jap. J. Appl. Phys. **19**, 2395 (1980).
 - [23] C. H. Seager, D. R. Tallant, J. Yu, and W. Götz, J. of Lumin. **106**, 115 (2004).
 - [24] Q. Yan, A. Janotti, M. Scheffler, and C. G. Van de Walle, Appl. Phys. Lett. **100**, 142110 (2012).
 - [25] G. Salvati, N. Armani, C. Zanotti-Fregonara, E. Gombia, M. Albrecht, H. P. Strunk, M. Mayer, M. Kamp, and A. Gasparott, MRS Interet J. Nitride Semicond. Res. **5S1**, W11.50 (2000).
 - [26] M. C. Tarun, M. Zafar Iqbal, and M. D. McCluskey, AIP Advances **1**, 022105 (2011).
 - [27] M. A. Reshchikov, K. Garbus, G. Lopez, M. Ruchala, N. Nemeth, and J. Nause, Mater. Res. Soc. Symp. Proc. **957**, 0957-K07-19 (2006).
 - [28] B. K. Ridley, J. Phys.: Condes. Matter **10**, L461 (1998).
 - [29] M. K. Kretov, I. M. Iskandarova, B. V. Potapkin, A. V. Scherbinin, A. M. Srivastava, and N. F. Stepanov, J. Lumin. **132**, 2143 (2012).
 - [30] G. E. Russel and C. C. Klick, Phys. Rev. **101**, 1473 (1956).
 - [31] F. Giustino, M. L. Cohen, and S. G. Louie, Phys. Rev. B **76**, 165108 (2007).